Process-based simulations of percolation from various landfill final covers in a cold climate

Alireza Amani[1], Marie-Amélie Boucher[1], Alexander Cabral[1], Vincent Vionnet[2], and Étienne Gaborit[2]

[1]Universite de Sherbrooke Departement de Genie Civil et de Genie du Batiment
[2]Environment and Climate Change Canada Montreal Office

May 28, 2023

Abstract

Accurate estimation of percolation is crucial for assessing landfill final cover effectiveness, designing leachate collection/treatment systems, and many other applications, such as in agriculture. Despite the importance, percolation is seldom measured due to the high cost and maintenance of lysimeters, underlining the need for skillful simulation. Process-based numerical models, despite requiring validation and numerous parameters, present an alternative for percolation simulation, though few studies have assessed their performance. This study compares percolation measured from three fully instrumented large-scale experimental plots to simulate percolation using a new version of the Soil Vegetation and Snow (SVS) land-surface model with an active soil-freezing module. Previous research indicates numerical model performance may significantly vary based on soil-related parameter values. To account for input data and parameter uncertainty, we use an ensemble simulation strategy incorporating random perturbations. The results suggest that SVS can accurately capture the seasonal patterns of percolation, including significant events during snowmelts in spring and fall, with little to no percolation in winter and summer. The continuous ranked probability skill score values for the three plots are 0.13, -0.13, and 0.33. SVS simulates near-surface soil temperature dynamics effectively (R 2 values 0.97-0.98) but underestimates temperature and has limitations in simulating soil temperature in snow-free situations in the cold season. It also overestimates soil freezing duration, revealing discrepancies in the onset and end of freezing periods compared to observed data. This study highlights the potential of land surface models for the simulation of percolation, with potential applications in the design of systems such as leachate collection and treatment. While the SVS model already provides an interesting outlook, further research is needed to address its limitations in simulating soil temperature dynamics during soil freezing periods.

Process-based simulations of percolation from various landfill final covers in a cold climate

Alireza Amani *, Marie-Amélie Boucher , Alexandre R. Cabral

Department of Civil and Building Engineering, Université de Sherbrooke, Sherbrooke, Quebec, Canada

Vincent Vionnet , Étienne Gaborit

Environmental Numerical Weather Prediction Research, Environment and Climate Change Canada, Dorval, Quebec, Canada

---

Abstract

Accurate estimation of percolation is crucial for assessing landfill final cover effectiveness, designing leachate collection/treatment systems, and many other applications, such as in agriculture. Despite the importance, percolation is seldom measured due to the high cost and maintenance of lysimeters, underlining the need for skillful simulation. Process-based numerical models, despite requiring validation and numerous parameters, present an alternative for percolation simulation, though few studies have assessed their performance. This study compares percolation measured from three fully instrumented large-scale experimental plots to simulate percolation using a new version of the Soil Vegetation and Snow (SVS) land-surface model with an active soil-freezing module. Previous research indicates numerical model performance may significantly vary based on soil-related parameter values. To account for input data and parameter uncertainty, we use an ensemble simulation strategy incorporating random perturbations. The results suggest that SVS can accurately capture the seasonal patterns of percolation, including significant events during snowmelts in spring and fall, with little to no percolation in winter and summer. The contin-

*Corresponding author
Email address: `alireza.amani@usherbrooke.ca` (Alireza Amani)

uous ranked probability skill score values for the three plots are 0.13, -0.13, and 0.33. SVS simulates near-surface soil temperature dynamics effectively (R^2 values 0.97-0.98) but underestimates temperature and has limitations in simulating soil temperature in snow-free situations in the cold season. It also overestimates soil freezing duration, revealing discrepancies in the onset and end of freezing periods compared to observed data. This study highlights the potential of land surface models for the simulation of percolation, with potential applications in the design of systems such as leachate collection and treatment. While the SVS model already provides an interesting outlook, further research is needed to address its limitations in simulating soil temperature dynamics during soil freezing periods.

Keywords: land-surface model; percolation; lysimeter; soil freezing; soil moisture; soil temperature; landfill final cover; ensemble simulation;

---

1. Introduction

Accurate estimates of deep percolation, the net amount of water percolating below the root zone (Bethune et al., 2008), are necessary for various practical applications. In landfill engineering, precise percolation estimates are critical for assessing the effectiveness of landfill final covers to design leachate collection systems properly. Leachate, a toxic liquid produced from percolated water interacting with waste, must be treated to prevent environmental harm such as groundwater and soil pollution (Kjeldsen et al., 2002).

Percolation estimates are vitally important in agricultural water management for optimizing irrigation, i.e. minimizing percolation and maximizing transpiration (Wang et al., 2012). Percolation is also associated with nitrogen leaching from agricultural soils (Xu et al., 2017), which threatens groundwater quality and has other adverse effects such as contributing to the eutrophication of water bodies (Carpenter et al., 1998), leading to harmful algal blooms and loss of biodiversity (Abdalla et al., 2019; Ascott et al., 2017; Smith et al., 2006). In groundwater management, percolation rates are important for understanding aquifer recharge and developing effective conservation and management strategies, particularly in regions with low precipitation and high water demand where unsustainable groundwater abstraction can occur (Finch, 1998a).

Lysimeters, such as pan lysimeters, are reliable and accurate for measuring percolation directly in the field (Bethune et al., 2008; Kahale & Cabral, 2022; Mijares & Khire, 2012). However, they can be expensive to install and maintain, requiring specialized labor and materials, as well as regular maintenance and monitoring. This renders other methods of estimating percolation appealing, in particular during the pre-feasibility and feasibility phase of the design process.

Process-based numerical models, which consider the physical processes governing the transport of water through soil, could offer an alternative to costly direct measurements, or complement them. These models can, for example, be used to better understand the underlying processes and variables influencing percolation (for instance through sensitivity analyses), as well as testing the impact of different scenarios. This can for instance help applications such as irrigation management and groundwater conservation. A process-based model can help to quantify the response of percolation to different management practices (Bethune et al., 2008) and climate change scenarios (Wang et al., 2018), among other sources of uncertainty.

However, using any particular numerical model presents at least two challenges. First, a large amount of field data from locations with diverse climatic and physical conditions is required to validate the model. Second, a large set of physical parameters is needed to describe the natural systems being modeled, and this requires specialized knowledge and/or measuring equipment (Finch, 1998b; Bethune et al., 2008). As a result, there are relatively few studies that have focused on local percolation simulations using process-based models. Despite these challenges, process-based numerical models are a potential option for estimating percolation because they can be used to simulate it for example at various spatial and temporal scales, under different climatic conditions, or considering different management scenarios.

Bethune et al. (2008) reported on a lysimeter experiment in Southeastern

Australia aimed at measuring percolation in an irrigated pasture under various conditions such as different combinations of water table depths, soil types, and ponding times as a result of surface irrigation. The analysis of experimental data led to the identification of influential governing variables for percolation, which in turn were used to develop a conceptual model. This model was subsequently tested against lysimeter and field-scale water balance data. The performance of the developed model was benchmarked against both a data-driven model and a calibrated process-based model, namely, artificial neural networks and HYDRUS-1D (Simunek et al., 2005). The conceptual model performed better than the data-driven and process-based models for most soil types while requiring fewer input data compared to the artificial neural network.

Benson et al. (2005) evaluated the simulations of percolations from two models, UNSAT-H (Fayer, 2000) and VADOSE/W (Krahn, 2004), against measurements from an instrumented experimental plot in a semi-arid climate (California, USA). UNSAT-H overestimated surface runoff, which led to the model underestimating percolation. On the contrary, VADOSE/W was able to estimate runoff relatively accurately. However, similarly to UNSAT-H, it underestimated percolation. The authors hypothesized that this issue could be related to the accuracy of saturated hydraulic conductivity as an input parameter to the models.

Using the measured percolation/runoff quantities from the same test plot of Benson et al. (2005), Bohnhoff et al. (2009) assessed and compared the performance of HYDRUS, LEACHM (Hutson & Wagenet, 1995), VADOSE/W, and UNSAT-H. The accuracy of all water-balance components was influenced by the accuracy of the runoff prediction. Runoff was estimated more accurately when precipitation was applied uniformly throughout the day, the surface layer was given a larger saturated hydraulic conductivity, and Brooks-Corey functions were employed to describe the hydraulic characteristics of the soils. Percolation was consistently underestimated by all models. A five to ten-fold increase in the laboratory-obtained saturated hydraulic conductivity of the soils improved the simulation of percolation.

Past research focusing on percolation simulation has typically been carried out in regions characterized by minimal annual rainfall, negligible to non-existent snow accumulation, and the absence of seasonal freeze-thaw cycles. This concentration of studies in such specific geographic and climatic contexts means that their findings may not translate effectively to different environmental conditions. For instance, in regions where snow accumulation and soil freezing are prevalent, these factors can significantly influence soil hydrology (Fu et al., 2018). These circumstances add complexity for numerical models.

Furthermore, widespread models, such as HYDRUS-1D which is often used in landfill final cover assessment, do not consider factors like snow and soil freezing. This could limit the comprehensiveness and applicability of their results when dealing with diverse and more challenging environmental conditions.

Previous studies on simulating percolation did not account for sources of uncertainty, such as meteorological input data uncertainty, and soil hydraulic parameters' uncertainty, which can significantly impact the performance of models, as shown by Bohnhoff et al. (2009). Probabilistic approaches, like ensemble simulation, can help estimate these uncertainties by generating a range of possible outcomes based on different input data and parameters. Ultimately, better estimating these uncertainties allows for more informed decision-making.

Another important limitation of earlier percolation studies is that they only compared total annual simulated and measured percolation volumes, rather than daily or sub-daily time series (Mijares & Khire, 2012). This temporal aggregation restricts our ability to detect differences in the temporal patterns of percolation. It also limits the identification of potential causes of differences between simulated and measured values.

In this study, we use the Soil, Vegetation, and Snow (SVS) land-surface model (Alavi et al., 2016; Husain et al., 2016) to simulate point-scale percolation from the bottom of three large-scale experimental plots (soil enclosures). These experimental plots are designed and built to evaluate the performance of three different landfill final covers. They are located in Southeast Quebec (Canada), a region with a warm-summer humid continental climate (Dfb), according to the Köppen classification (Peel et al., 2007). Four pan lysimeters (two inside one of the plots) are installed to collect percolation, which is recorded hourly by data loggers.

SVS is a process-based model developed and used operationally by Environment and Climate Change Canada (ECCC), with a special focus on the representation of subsurface hydrological processes. SVS explicitly considers and simulates the processes related to the water and energy balance and snowpack evolution. Recently, a new soil freezing module has been added to the model, using the simple heat-conduction algorithm of Hayashi et al. (2007). SVS including this new soil freezing scheme sets apart from other models commonly used in percolation-related research, which do not account for snow and frozen ground on their own and require evapotranspiration as input data and makes it particularly appealing in cold climates. Previous works involving SVS have mainly focused on surface energy and water balance simulations (Maheu et al., 2018; Leonardini et al., 2020), and on SVS snowpack simulations (Leonardini et al., 2021).

With this work, we aim to address the following research question: are land-surface models (and in particular SVS) able to simulate percolation in a cold climate where the soil undergoes seasonal freeze-thaw cycles? We hypothesize that SVS will be able to simulate percolation from our three experimental plots, since it can account for the influential underlying processes, including soil freezing. To provide a more stringent performance assessment, we do not calibrate SVS using any field-measured data, which are typically unavailable to modelers. Instead, we use an ensemble simulation approach, to account for uncertainties related to meteorological input data, input parameters such as soil hydraulic/thermal properties, and uncertainties related to the choice of the lower-boundary condition of SVS that directly influences percolation simulation. The work presented in this study is the first to evaluate the performance of SVS regarding percolation simulations and soil hydrology in a cold climate. Moreover, it is the first study involving the newly developed soil-freezing module and assessing its performance.

The remainder of this paper is structured as follows: In Section 3, we provide a brief description of the SVS land-surface model and the experimental setup. In Section 2 we present the case study, including a description of the experimental site and the available data. In Section 4, we present and discuss the results. Finally, in Section 5, we summarize the main findings of the study, discuss the implications and limitations of our work, and suggest directions for future research.

2. Case study

2.1. Experimental plots

Figure 1 shows the configuration of the three experimental plots (enclosures). The plots are constructed at the St-Nicéphore landfill site in Drummondville, Quebec (Canada), shown in Figure 2. These experimental plots are constructed as prospective landfill final covers where the main variable of interest is the percolation exiting through these covers into the waste layer.

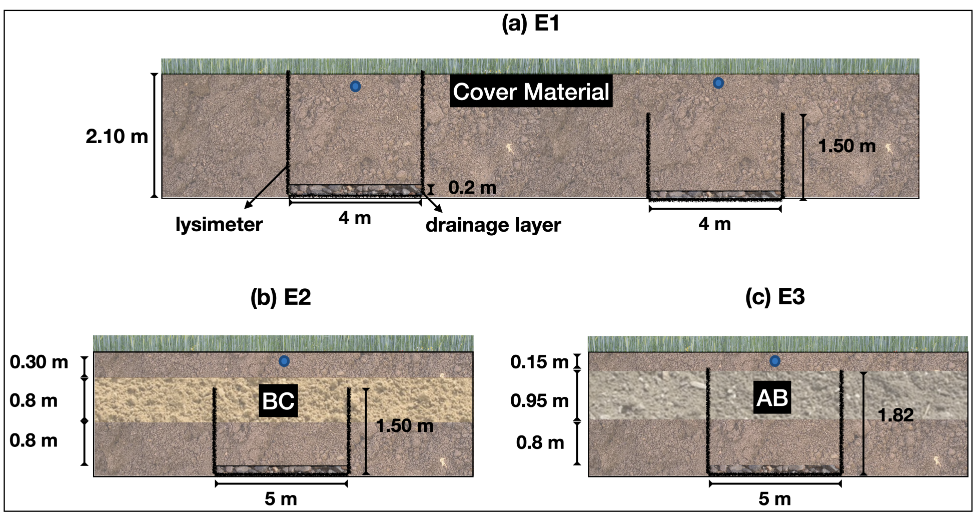

Figure 1: The different soil layers in the three experimental plots. The blue circles represent the soil moisture/temperature sensors placed at 7.5 cm depth.

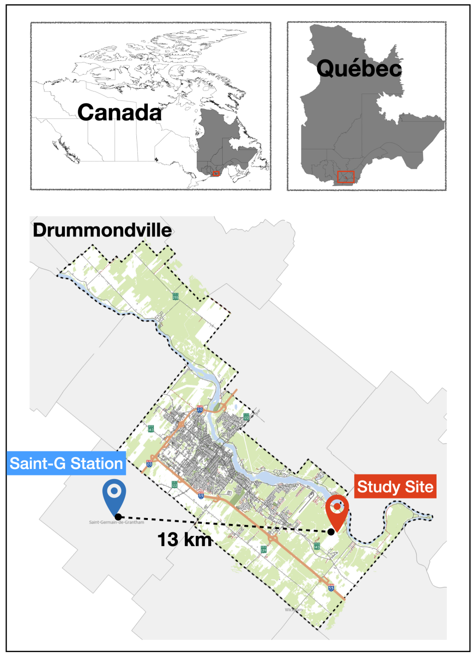

Figure 2: The location of the study site and the Saint-Germain de Grantham weather station on the map

The percolation from the bottom of these plots is collected using pan lysimeters and recorded hourly using tipping counters (100 ml for each tip) (Figure 3-a). Soil water content and soil temperature are also measured (half-hourly) using dielectric sensors (5TM made by Decagon Devices Inc) depicted as blue circles in Figure 1. These sensors are placed at a depth of 7.5 cm. The plots are equipped with several more sensors and instruments (e.g. settlement plates), not shown in the figures since they are not used in this study.

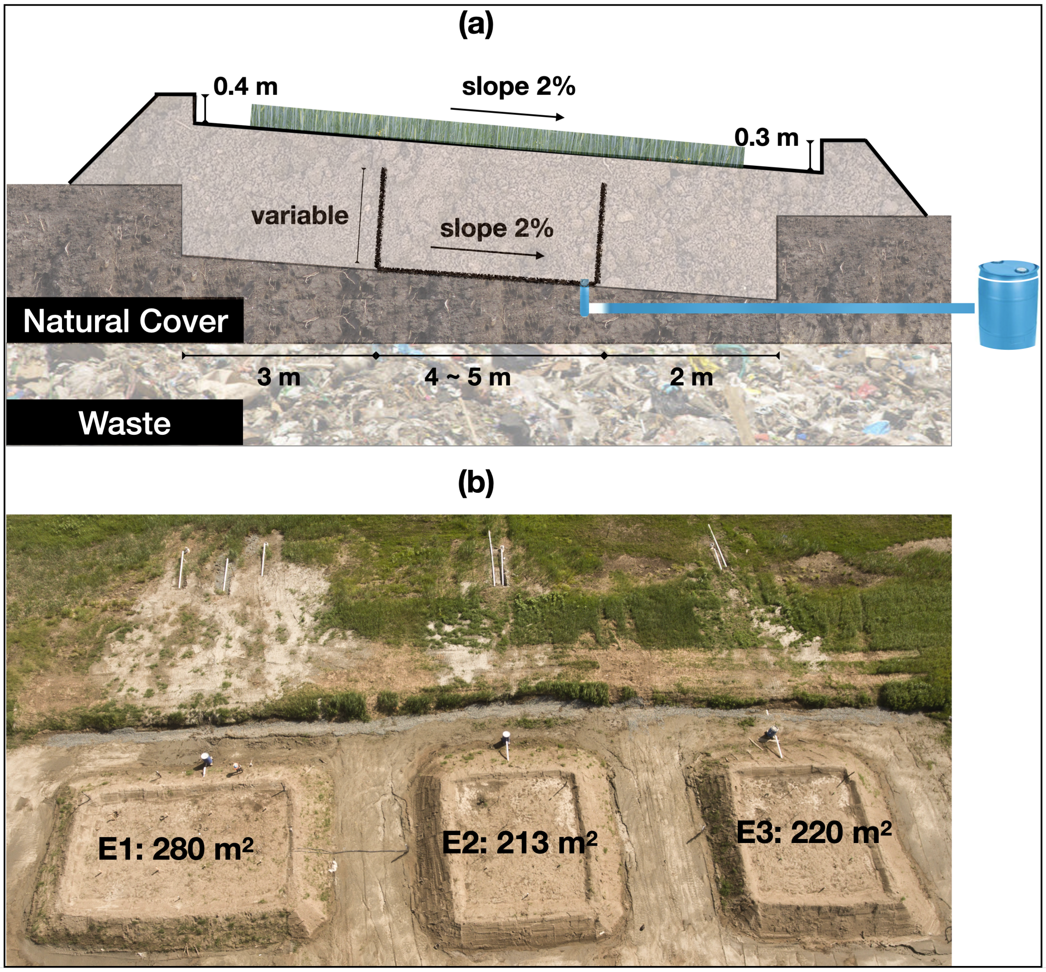

Figure 3: The cross-section view of the experimental plots (a) and the top-view of the plots in the site immediately after construction in the summer of 2018 (b)

Each experimental plot has a different configuration of soil layers. The E1 plot 1-a contains exclusively typical cover material, a term adopted to refer to a type of soil, ranging from sandy to silty, commonly used as cover materials at St-Nicéphore landfill. The E2 plot 1-b includes a layer of BC soil and two layers of cover material, and E3 has a layer of AB soil between layers of cover material. BC and AB refer to the level of contamination according to the local legislation. At the bottom of each lysimeter, an identical 20-cm drainage layer of sand and gravel is placed to facilitate the draining of the water from the bottom of the lysimeters. Table 1 presents the laboratory-obtained parameters for the aforementioned soils. Section 3.4 describes how these parameters were measured in the laboratory.

2.2. Data

The long-term precipitation records for the study site (Drummondville) indicate this location, on average, receives more than 1050 mm of precipitation (snowfall + rainfall), including 227 cm of snowfall annually. Snow depth measurements from 1982 to 2017 show that on average there are 109 days with more than 3 cm of snow on the ground.

The meteorological forcing variables for SVS are obtained from the Saint-Germain de Grantham (Saint-G) weather station (13 km from the study site, see Figure 2), except for short-wave and long-wave radiation that is not measured anywhere nearby. Radiation from the ERA5 reanalysis (Hersbach et al., 2020) is used as a proxy. Specific humidity is estimated using dew point temperature and atmospheric pressure. The Saint-Germain de Grantham station is equipped with a double Alter Shield precipitation gauge and as suggested by Smith et al. (2022) no wind-bias-adjustment is applied to the precipitation data.

The precipitation's phase discrimination in SVS is done using a zero-degree threshold. However, we overwrite this by using the formula proposed by Jennings et al. (2018) which distinguishes between rainfall and snowfall using humidity and air temperature, as in equation 1

$$P_{snow} = \frac{1}{[1 + \exp c_1 + (c_2 T_a) + (c_3 R_h)]} \tag{1}$$

where T_a is air temperature (°C), R_h is the relative humidity (%), and c_1, c_2, c_3 are empirical coefficients which are equal to -10.04, 1.41, 0.09, respectively. Precipitation is recognized as snow if P_{snow} is greater than 0.5, and rain otherwise.

Table 1: The laboratory-obtained properties of the soil layers inside the experimental plots

			Soil Parameters						
	Sand	Clay	W_{sat}	W_{fc}	W_{wilt}	K_{sat}	ρ_d	ψ_a	b
Soil	(%)	(%)	(m^3/m^3)	(m^3/m^3)	(m^3/m^3)	(m/s)	(g/cm^3)	(kPa)	(-)
Cover material	55–78	5–12	0.29–0.33	0.05–0.09	0.02–0.06	7×10^{-6}–5.4×10^{-5}	1.46–1.69	0.26	3.9
BC	84	3	0.31	0.17	0.15	4.4×10^{-6}–4.9×10^{-5}	1.55–1.72	0.35	7.8
AB	26	10	0.28	0.20	0.17	4×10^{-7}–4.6×10^{-6}	1.54–1.64	0.33	11.6

3. Methods

3.1. SVS land-surface model

The SVS land-surface model is developed and is actively maintained by ECCC (Alavi et al., 2016; Husain et al., 2016; Leonardini et al., 2021). It requires seven hourly meteorological variables as input data, including air temperature, short- and long-wave radiation, wind speed, specific humidity, atmospheric pressure, and precipitation. To start SVS under snow-free conditions, initial values for soil volumetric water content and soil temperature must be provided for each defined soil layer. By default, SVS estimates soil hydraulic and thermal properties using pedo-transfer functions based on the percentage of sand and clay in each layer. Therefore, these two parameters are the only ones that are required to fully describe the soil column in SVS.

Each grid cell in SVS can be divided into four tiling components: 1) bare ground, 2) low/high vegetation, 3) snow over bare ground and low vegetation, and 4) snow under high vegetation. For each of these four components, SVS uses the force-restore approach (Bhumralkar, 1975; Blackadar, 1976) to calculate the energy budget. SVS uses a one-layer approach for the snowpack and the vegetation canopy. A detailed description of the SVS snow component is presented in Leonardini et al. (2021).

Within the soil column, the vertical movement of water is governed by Richards equation for unsaturated flow, solved by a finite difference scheme (Verseghy, 1991). In SVS, the soil water retention curve (SWRC) and vertical hydraulic conductivity (K_v) are modeled using the following two equations (Clapp & Hornberger, 1978):

$$\psi(z,t) = \psi_a \left[\frac{\omega(z,t)}{\omega_{sat}}\right]^{-b} \tag{2}$$

and

$$K_v(z,t) = K_{v,sat} \left[\frac{\omega(z,t)}{\omega_{sat}}\right]^{2b+3} \tag{3}$$

where ψ (kPa) is soil suction, ω_{sat} is the saturated soil volumetric water content, and $K_{v,sat}$ is the saturated vertical hydraulic conductivity of the soil. In equations 2 and 3, b and ψ_a are empirical (fitting) parameters related to the slope of the SWRC and air-entry value suction of the soil, respectively.

In SVS, by default, percolation at the bottom of the last soil layer is calculated only when the soil volumetric water content is larger than the water content at field capacity. We refer to this parameter as ω_{trig}. Furthermore, the calculation of surface runoff in the model is based on the saturated fraction of the surface and is generated when either the precipitation rate is larger than the first layer's $K_{v,sat}$ or when soil moisture exceeds saturation.

The default version of SVS does not simulate soil freezing and thawing and its impact on infiltration and percolation (Alavi et al., 2016). To overcome this limitation, a simple soil freezing scheme has been implemented in SVS. It relies on the simple heat-conduction algorithm of Hayashi et al. (2007) and is described in detail in Appendix A.

3.2. Experiment design

3.2.1. Research question

Our research question is **are land-surface models (and in particular SVS) able to simulate percolation in a cold climate where the soil undergoes seasonal freeze-thaw cycles**? To address this question, 200-member ensembles are created for each plot to account for uncertainties in the model's meteorological input data, input parameters related to soil hydraulic properties, and lower boundary condition related to the simulation of percolation.

The construction of experimental plots was concluded in the summer of 2018, however, the field data (i.e. percolation + soil moisture/temperature) for the first year after the construction is not used in the analysis due to the impacts of experimental plot stabilization. Meteorological data for this period, July 2018 to July 2019, is used for model warm-up. The model evaluation period spans from July 2019 to the end of June 2021. The vertical discretization of the soil column inside SVS is identical for the three plots and is as follows: the first and last 15 cm of the 190 cm long soil column is divided into layers of 2.5 cm, the rest of the soil column is divided into layers with 5 cm depth (total of 44 layers for each soil column).

3.2.2. Constructing the ensembles

To represent the uncertainty related to the model's input parameters, a sampling interval is considered for the parameters in Table 1 for which there are several laboratory-estimated values. The interval is the same as the range presented in the table for each parameter.

The interval for ω_{trig} is defined as a multiplier from 0.5 to 0.99 of ω_{sat} of the corresponding soil layer, which we argue is a reasonable range considering the capillary effect present at the interface between the soil covers and the drainage layer (made of sand and gravel). To ensure a more evenly distributed sample, we use Latin hypercube sampling (Loh, 1996) to create the ensemble members rather than random sampling.

The ensemble of meteorological data is constructed by applying a random perturbation to the variables and following the approach proposed by Charrois et al. (2016), which ensures physically consistent temporal variations for the data. According to this approach, a first-order autoregressive model, 4, is used to compute the random perturbation for each variable (Deodatis & Shinozuka, 1988).

$$P_t = \phi P_{t-1} + \epsilon_t \tag{4}$$

In Eq. 4 P_t is the perturbation value at time t, ϕ is the parameter for the autoregressive model, and ϵ is a white noise process with zero mean and σ^2 variance. ϕ is obtained by fitting an AR(1) model to the time series of each variable and variance σ^2 is computed using the standard deviation of the residuals between the variables from the Saint-Germain de Grantham station and the corresponding variable from the field stations (average of three stations) following Eq. 5.

$$\sigma^2 = \sigma_{res}(1 - \phi^2) \tag{5}$$

An additive perturbation is applied to air temperature, dew temperature, and atmospheric pressure. A multiplicative perturbation is applied to shortwave radiation, wind speed, and relative humidity Charrois et al. (2016). The multiplicative perturbation is limited to [0.8, 1.2] to avoid extreme values.

Concerning longwave radiation, as there is no field measurement available, no perturbation is applied. Precipitation data is perturbed according to the World Meteorological Organization's recommended range of uncertainty for rainfall measurements taken by automatic tipping-counter rain gauges, which is ± 5 % (Lanza et al., 2005; Colli et al., 2013). The phase of precipitation is computed following the perturbation of air temperature and relative humidity data.

3.3. Performance assessment metrics

The performance of the ensembles regarding different hydrological variables, namely the soil moisture/temperature, snow depth, and percolation, is evaluated using the Continuous Ranked Probability Score (CRPS) (Bröcker & Smith, 2007). The CRPS is a widely-used metric that penalizes the over or under-dispersion and bias in ensemble simulations (Clark, 2017); a low CRPS denotes better simulations, and perfect simulations would have a score of zero. The *ensverif* Python library: `https://pypi.org/project/ensverif/` is used to calculate the CRPS.

We use the Continuous Ranked Probability Skill Score (CRPSS) to compare the simulations produced by SVS to a benchmark. The CRPSS is calculated using Eq. 6. A positive CRPSS indicates that SVS performs better than the benchmark, a negative value means that it performs worse, and a CRPSS of zero indicates that there is no difference in performance between the two. A CRPSS of 1 signifies a perfect simulation.

$$CRPSS = 1 - \frac{CRPS_{svs}}{CRPS_{bench}} \tag{6}$$

To have realistic and competitive benchmarks, we linearly varied the observed values between $\bar{y}_{obs} - \frac{s_{obs}}{4}$ and $\bar{y}_{obs} + \frac{s_{obs}}{4}$ and assigned each of them to an ensemble member (200 total). Here, $\bar{y}_{obs}$ is the average value for the observations of the hydrological variable, and s_{obs} is the standard deviation of the observations.

We also use R^2 (square of Pearson's correlation coefficient) and mean-bias-error (MBE) to assess the performance of the ensemble average regarding the variables of interest. MBE is calculated by subtracting the observations from simulated values.

3.4. Laboratory methods

The soil water content at saturation, field capacity, and the wilting point are obtained by conducting the HYPROP (HYdraulic PROPerty analyzer, Schindler & Müller, 2017; Schindler et al., 2015) technique (METER Group, Inc.). This technique involves measuring the pressure head, against time, at two different depths within a 5-cm soil column. This is done while the water evaporates from the surface. Fluxes and water contents are determined by continuous weighing of the column. In the end, the measurements for pressure head, water content, and evaporation fluxes are used to obtain the water retention curve which is a graph that shows the relationship between the soil's water content and the soil suction (Bezerra-Coelho et al., 2018).

Based on the HYPROP results, the soil volumetric water content at field capacity (ω_{fc}) for the different types of soils is estimated to be the soil water content corresponding to the 33 kPa suction. The b coefficient and ψ_a in Eq. 2 are obtained by fitting the equation to water content and suction measurements that have been obtained using the HYPROP technique. This is done using a mathematical optimization algorithm called the Levenberg-Marquardt algorithm, which adjusts the parameters to find the best fit between the equation and the measurements.

The saturated hydraulic conductivity (K_{sat}) was estimated using the KSAT (METER Group, Inc.) device, which automatically measures K_{sat} of saturated soil samples based on Darcy's equation. In this test, a fully saturated soil sample is percolated with degassed water at room temperature, perpendicular to the sample's cross-section. During the percolation, the flow rate and hydraulic gradient are measured. K_{sat} $(m.s^{-1})$ is then calculated using Darcy's equation:

$$K_{sat} = \frac{LV}{\Delta H A \Delta T} \tag{7}$$

where ΔT is the length of the time interval (s), V is the volume of water passed through the sample (m^3), L is the length of the soil sample (m), A is the soil sample cross-sectional area (m^2), and ΔH is the hydraulic head gradient along the flow direction (m).

4. Results and discussion

Figure 4 presents the CRPSS, CRPS, MBE, and R^2 values obtained by SVS (2019-07-01 to 2021-06-30) for the ensemble simulation of daily averaged surface soil moisture/temperature and daily percolation volumes for the three experimental plots. For the E1 experimental plot, the metrics values represent the mean calculated from two separate sets of observations for each variable.

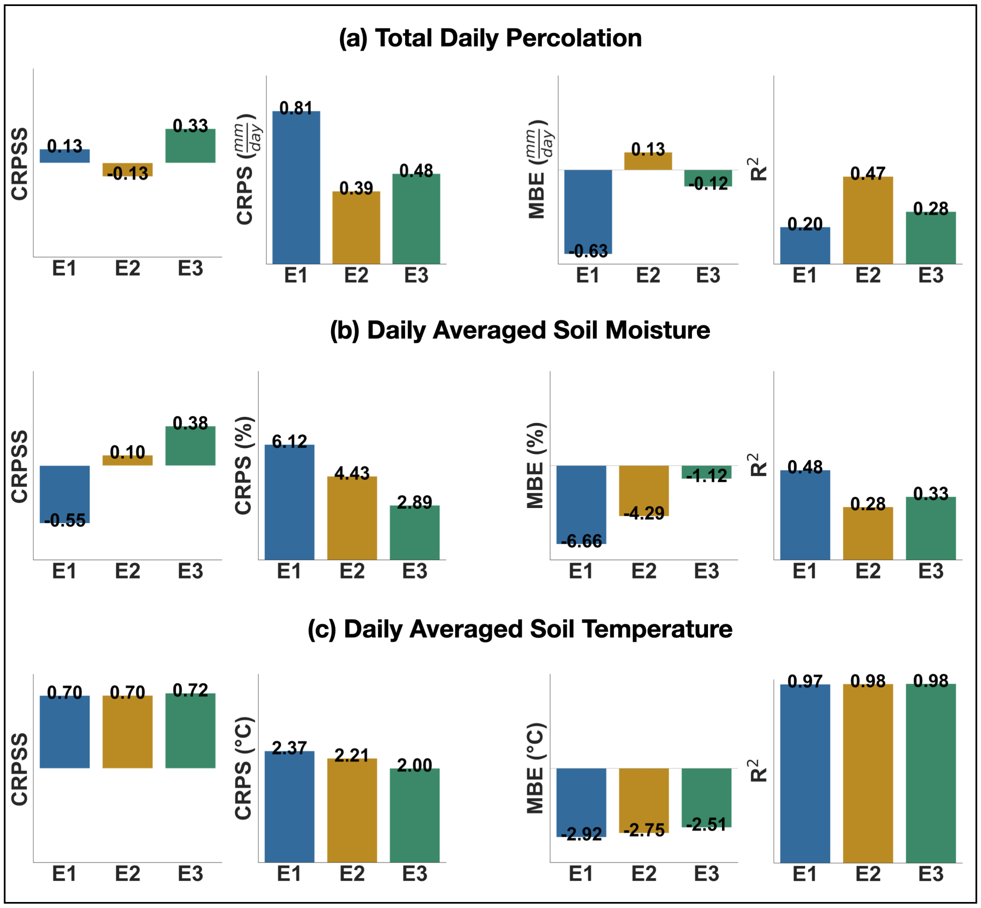

Figure 4: Performance assessment metrics for assessing the performance of SVS ensemble simulation (CRPS and CRPSS) and ensemble mean (MBE and R^2) concerning the experimental plots and soil moisture/temperature (7.5 cm) and percolation. There are two independent measurements available for E1.

In the following subsections, we further analyze the performance of SVS for the simulation of snow, soil temperature and soil moisture, and percolation. To gain insight into the general quality and realism of the model, its performance regarding the simulation of snow cover and soil freezing is assessed before assessing the quality of the simulation for percolation.

4.1. Snow simulation

Figure 5 shows the comparison between the snow depth measured by the Saint-Germain de Grantham weather station (blue line) and the values simulated by SVS (in orange) for two consecutive winters (Nov-May). The blue triangles represent manual on-site snow depth measurements. Each point represents the average of 10 samples taken on a specific day. These measurements are indicative of the similarity between the snow depth at the Saint-Germain de Grantham station and the actual snow cover on site.

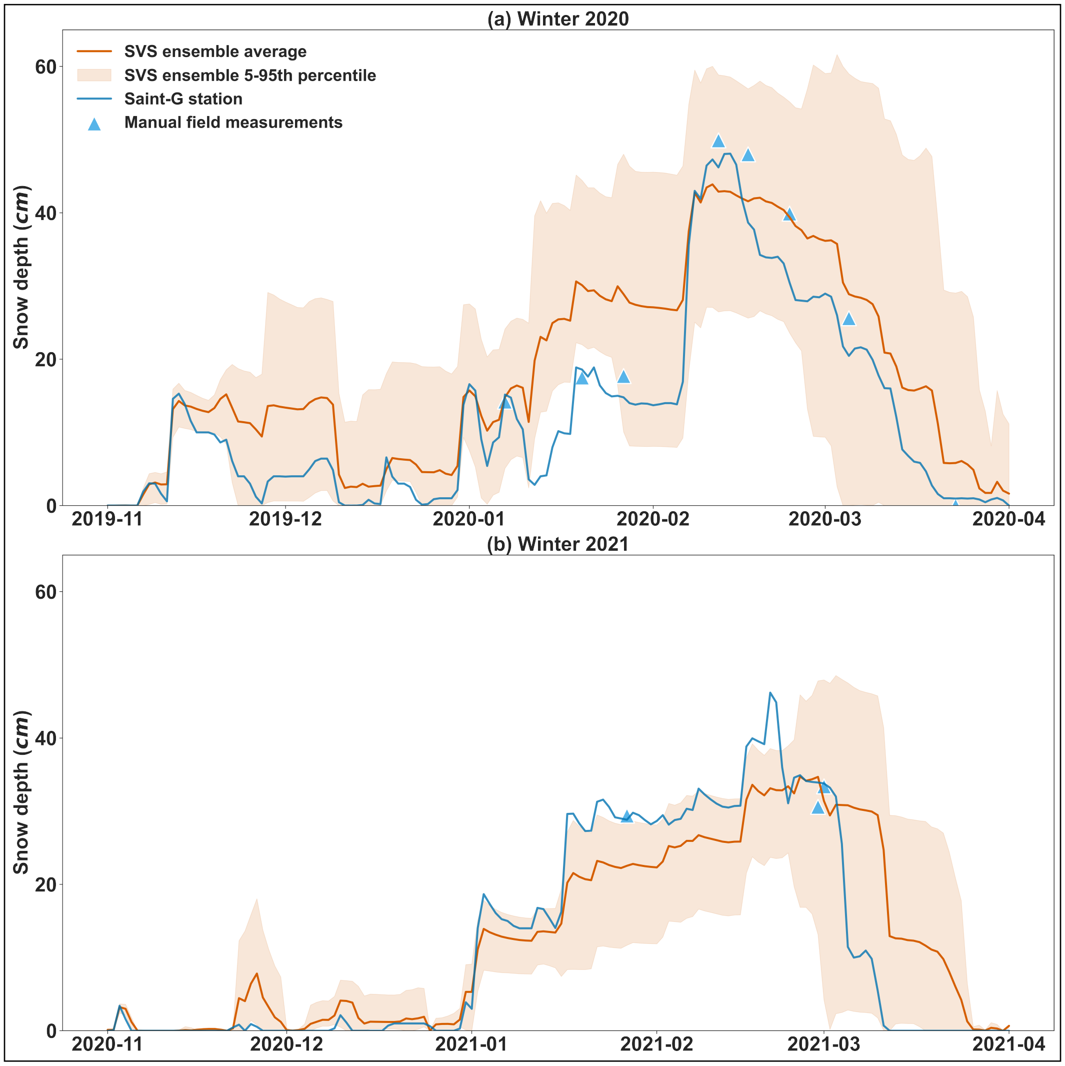

Figure 5: Snow depth values measured by the Saint-Germain de Grantham weather station (blue line) and simulated by the SVS model (shown in orange as the ensemble mean and 5-95th interpercentile range) for a) the winter of 2020 and b) the winter of 2021. The triangles are on-site manual snow measurements.

The simulated snow accumulation and melt during the two winter periods are generally consistent with the observations and SVS performs well in this regard, which is reflected by a CRPSS of 0.67 and R^2 of 0.82 (average over two winters). The ensemble simulation can be considered reliable since the observed snow depth measurements reside within the ensemble for most of the two winters, denoting that ensemble simulations are successful at capturing the uncertainty associated with the snow melt and accumulation process.

The good performance of SVS in the simulation of snow cover is vital for simulating snowmelt events in the spring, which can result in significant percolation volumes. However, the model's ability to simulate the resulting percolation is largely dependent on its simulation of the soil freeze-thaw cycle, as soil freezing impacts the infiltration capacity of the soil. SVS's performance in simulating near-surface soil temperature will be discussed in the following section.

4.2. Soil temperature at 7.5 cm

Figure 6 shows the simulated soil temperature values from SVS (in red) and the temperature values recorded by sensors at a depth of 7.5 cm within the plots (shown in light/dark blue).

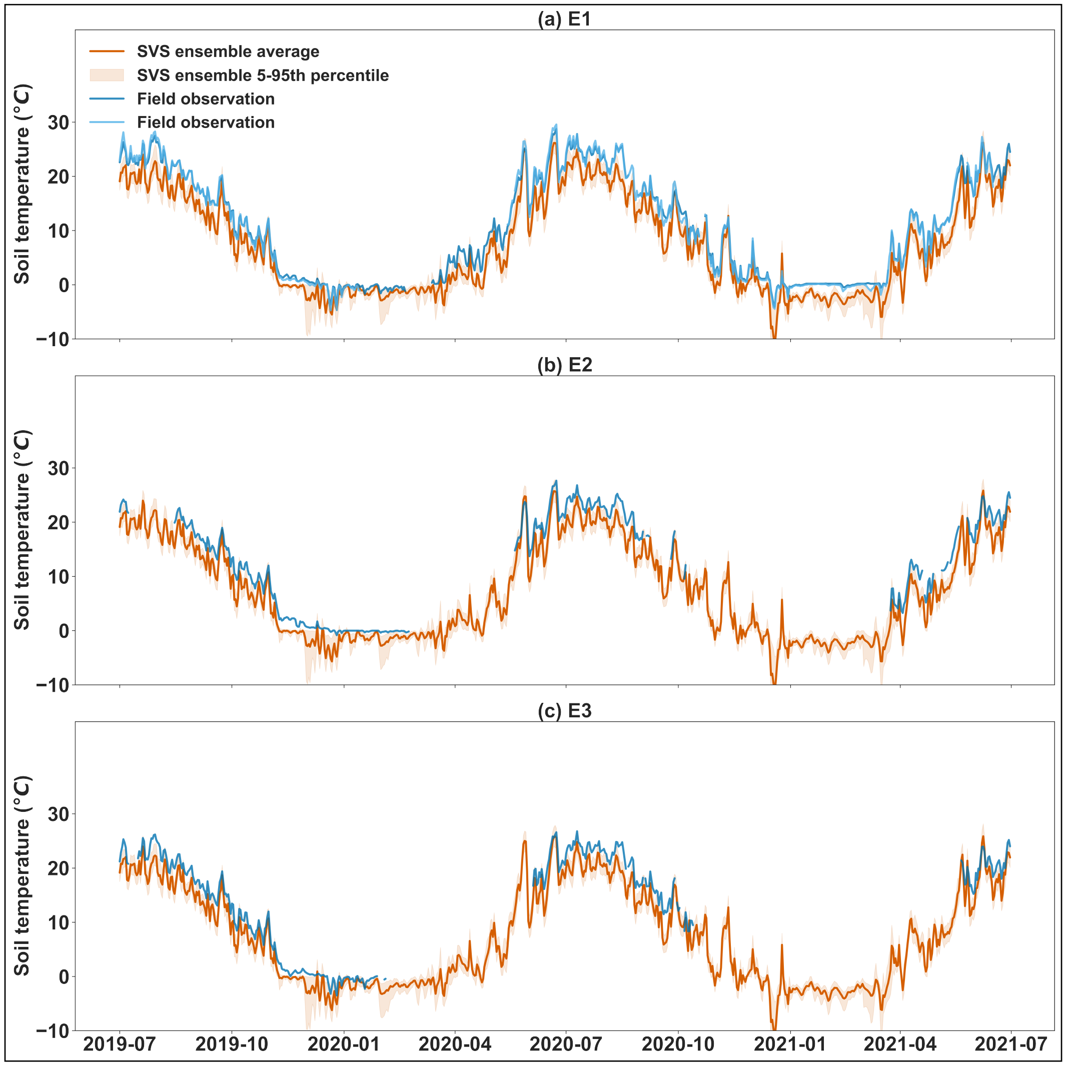

Figure 6: Daily averaged soil temperature simulation by SVS (in orange, with the ensemble mean and the 5-95th percentile range) and temperature values from a sensor (in light/dark blue) placed at 7.5 cm depth of the (a) E1, (b) E2, (c) E3 plots. Two sensors were placed inside the E1 plot

Figure 6 shows that SVS simulates the near-surface soil temperature reasonably well, for all plots and throughout the year. As shown in Figure 4, the ensemble has a CRPSS of around 0.70, and the ensemble average has R^2 of about 0.98 for all three plots, indicating a strong agreement between the simulation and observations. This demonstrates the model's ability to effectively capture the seasonal dynamics of near-surface soil temperature. The similarity of values for the evaluation metrics between all plots is because the near-surface soil is the same for all plots, i.e. cover material (Table 1).

The MBE values for the ensemble mean are -2.92, -2.75, and -2.51 °C for the E1, E2, and E3 plots respectively. These values indicate that SVS tends to underestimate near-surface soil temperature. The underestimation issue is more pronounced at a few specific periods, for instance, Dec-2020, Dec-2021, and Mar-2021, as shown in Figure 6, where most or all ensemble members significantly underestimate soil temperature (or overestimate frost depth).

Figure 6 also shows that the ensemble has a low spread, especially for non-freezing temperatures. On one hand, this can indicate a robust performance by SVS which exhibits low sensitivity to the perturbation concerning input data and parameters (see Section 3.2.2) in the simulation of near-surface soil temperature. On the other hand, this can indicate an overconfident ensemble, leading to the underestimation of underlying uncertainty affecting the soil temperature. The latter point might be related to the fact that the uncertainty concerning the soil thermal parameters, such as soil (solid and dry) thermal conductivity, is not directly explored in the construction of the ensemble. In the ensemble, the perturbation of soil sand/clay content, porosity, and dry density is responsible for variations in the thermal properties of the soils, as SVS uses those parameters to estimate soil thermal conductivity.

It is also important to determine how well the model simulates the onset, duration, and end of soil freezing, with particular emphasis on the latter, which often coincides with the melting of accumulated snow and is a major hydrological event in areas with significant snow accumulation (Iwata et al., 2010). For the analysis, we only use data from one of the sensors inside the E1 plot, the dark blue line in Figure 6-a, since it is the source of soil temperature observations for which we have the fewest number of missing values for both winters. We compare the observations with the ensemble mean. It is reasonable to assume that the analysis would be very similar for E2 and E3 since their near-surface soil has the same type as E1 (i.e. cover material).

During the first winter (2019-11-01 to 2020-04-01), there are 132 days with observations, with a daily-averaged observed soil temperature of 0.55 °C. The simulated average soil temperature is -1.06. For this period, the soil at a depth of 7.5 cm is frozen for 60 days, whereas for the ensemble mean (simulations), this number is 113. The freezing period starts on 2019-12-13 according to the sensor, while according to the simulations, it begins more than one month earlier, on 2019-11-09. It is difficult to compare the end date of the freezing period between observations and simulations, as the period between 2020-02-21 and 2020-03-12 is missing from the observations. Nevertheless, the observations from 2020-03-12 onward show positive values, while the average freezing period according to the simulations ends on 2020-03-25.

During the second winter (2020-11-01 to 2021-04-01), there are 151 days of available observations, with a daily averaged observed soil temperature of 1.42 °C, compared to -1.05 °C for the simulations. The observation record shows that there are only 37 days where the soil is frozen at 7.5 cm. The simulation shows a significantly larger number, with a total of 113 days where the soil is frozen. The first subzero day according to the simulations is on 2020-11-01, while for the observations it is on 2020-12-16. The last frozen day according to the simulation is on 2021-03-22, while for the observations it is on 2021-03-17.

Examining the simulated snow depth values for the ensemble median suggests that the severe underestimation of surface soil temperature occurs when there is little to no simulated snow cover. Snow cover acts as an insulator for the underlying soil and is inversely related to frost depth, an effect considered in the calculation of surface layer heat flux in SVS (Appendix A). The Saint-Germain de Grantham weather station's snow depth measurements also show little or no snow cover during these periods, indicating that the underestimation of soil temperature is unlikely caused by an underestimation of snow cover in the model.

This suggests that the soil freezing module of SVS may not perform well in simulating soil temperature for snow-free situations and air temperatures below the freezing point. This may be associated with the fact that the soil freezing scheme is used as an upper boundary condition for the surface temperature from the force restore scheme implemented in SVS Husain et al. (2016).

This scheme neglects the effects of soil freezing and thawing (latent heat release) on its prognostic temperature variables. Boone et al. (2000) have shown how the inclusion of these effects in a force restore scheme can improve the simulation of soil temperature when the soil freezes. Neglecting this effect in SVS may lead to an underestimation of the surface soil temperature during the fall in snow-free conditions affecting the ground heat flux used as the upper boundary conditions for the soil freezing scheme and ultimately generating an overestimation of the frost depth. In addition, the soil freezing dynamic in the fall depends on the liquid water content in the soil at that period (Zhao et al., 1997; Kurylyk & Watanabe, 2013).

The next section we will specifically focus on assessing the accuracy and reliability of SVS's soil moisture simulation, which is equally important for understanding hydrological processes in snow-dominated areas.

4.3. Soil moisture at 7.5 cm

The accuracy of a model's simulated overland flow can often be assessed by examining its simulated near-surface soil moisture, which can provide an indirect way to evaluate the model's performance in cases where there are no direct measurements of overland flow available. Figure 7 displays the simulated soil moisture values from SVS (in orange) and the moisture values recorded by sensors at a depth of 7.5 cm within the experimental plots in (dark/light) blue.

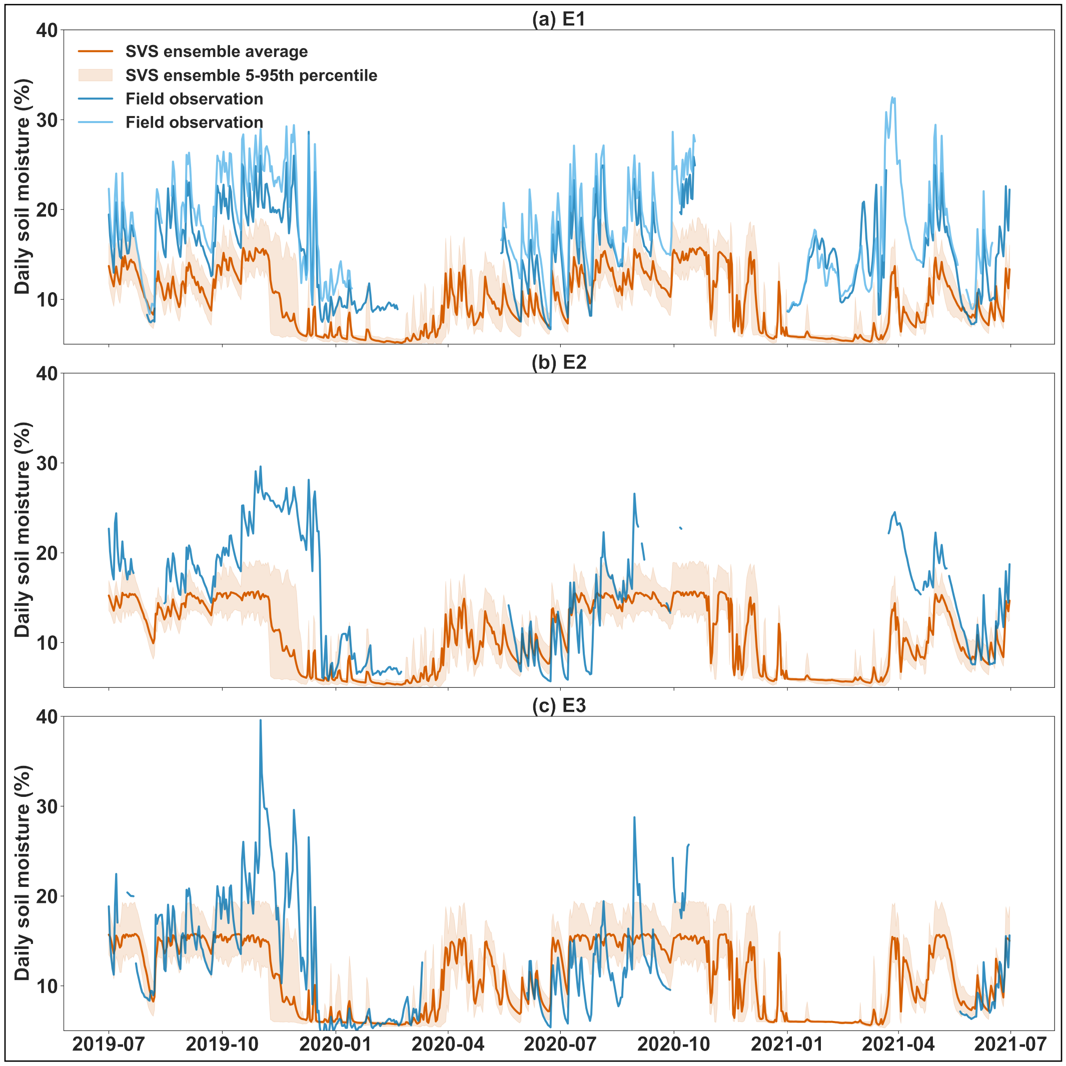

Figure 7: Daily averaged soil moisture simulation by SVS (in orange, with the ensemble mean and the 5-95th percentile range) and moisture values from sensors (in light/dark blue) placed at 7.5 cm depth of the (a) E1, (b) E2, (c) E3 plots. Two sensors were placed inside the E1 plot.

Concerning the E1 experimental plot, Figure 7-a shows that SVS is consistently underestimating (i.e. negative bias) soil moisture at 7.5 cm, which is more conspicuous after snowmelt events, for instance in Nov 2019, Dec 2019, and Mar 2021 (see Figure 5). The mean-bias-error (MBE, simulation - observation) between the ensemble mean and the two sensors are -5.5 % and -7.83 %.

The negative bias is very likely the reason why SVS has negative CRPSS values, -0.37 and -0.73 concerning the first and second moisture sensors, which means it performs worse than the simple benchmark. This is in turn due to the low reliability of the ensemble. The lack of reliability in the ensemble is primarily attributed to its inability to consistently encompass the observations within its range for the majority of the time steps. Using the decomposition proposed by Hersbach (2000), the total CRPS of 7.2 % for SVS (concerning the second sensor) can be decomposed into reliability and potential components of 7.07 % and 0.13 % respectively. This demonstrates the fact that most of the total CRPS is due to the low reliability of the ensemble.

Results shown in Figure 7 highlight an underestimation of the soil liquid water content in the fall that can partially explain why the soil freezes too quickly in SVS. It is also possible that the issue may be exacerbated due to the uncertainty present in the radiation data used to drive SVS, which directly affects the soil heat transfer calculations (the shortwave and longwave radiation data are obtained from the ERA5 dataset as long-term direct observations are not available). Such bias in the radiation forcing may explain why the soil temperature is also underestimated during the warm period.

The weak performance of the ensemble simulation, as measured by the CRPSS, can be partially attributed to a large discrepancy between the laboratory-obtained ω_{sat} of the near-surface soil, cover material, and the actual values deduced from analyzing half-hourly moisture measurements. The largest value obtained in the laboratory is 33 % (see Table 1), while the two sensors inside the E1 plot have recorded values around 38%. This means the actual ω_{sat} (and porosity) of cover material used inside E1 can be at least 15 % larger than the laboratory-obtained value. Since cover material is used for the near-surface soil of all of the plots, we should expect a similar discrepancy affecting the performance of SVS concerning E2 and E3. In the case of E2, the moisture sensor has recorded a value of 37 %, and the sensor placed inside E3 has recorded a value of 44.9 % (a storm event in Aug 2020)

The above-mentioned issue might be related to the fact that all laboratory tests of soil hydraulic parameters were conducted during the construction phase of the experimental plots. After construction (summer of 2018), these plots continued to experience settlement as well as soil freeze-thaw cycles, and this can significantly impact soil hydraulic properties, such as porosity and saturated hydraulic conductivity. This process is disruptive and is expected to increase these properties through the expansion of water in soil pores (as it freezes into ice) and rearrangement of soil particles (Rooney et al., 2022; Xu et al., 2021). The resulting increased porosity leads to a larger area for water flow, contributing to an expected increase in saturated hydraulic conductivity.

SVS's overestimation of the soil freezing period (Section 4.2), which begins earlier and lasts longer than suggested by the sensor data, could be another contributing factor to its underestimation of soil moisture. During these extended periods of simulated soil freezing, water infiltration would be reduced according to simulations, potentially leading to lower modeled soil moisture levels, which is more critical at the beginning of the spring and during snowmelt events.

Concerning the E2 and E3 plots, Figure 7-b, c, shows that, despite the aforementioned discrepancy, SVS performs better than the benchmark simulation, with CRPSS values of 0.10 and 0.38, respectively. This could be partially because the sensors inside E2 and E3 have missing values for most of the winter and spring of 2021, a period when the performance of SVS degrades, in the case of the E1 plot (see Figure 7-a).

Despite the negative CRPSS values for SVS regarding the E1 plot, Figure 7-a demonstrates that SVS adequately captures the overall seasonal and subseasonal variations in near-surface soil moisture. This trend is similarly observed for the E2 and E3 plots (Figure 7-b, c). In the case of E1, this is also evident in the R^2 values of around 0.48, which is moderately high considering the fact that R^2 between the two adjacent soil moisture sensors inside E1 (within a few meters) is 0.85. This demonstrates the inherent variability and uncertainty in the observed soil moisture measurements themselves, a consideration that affects the assessment of the model's performance.

In the next section, we examine the model's performance in simulating percolation, which is our ultimate goal.

4.4. Daily percolation

Figure 8 shows the simulated volumes of daily percolation (in orange) and the percolation volumes collected by the pan lysimeters at the bottom of the experimental plots (in light/dark blue).

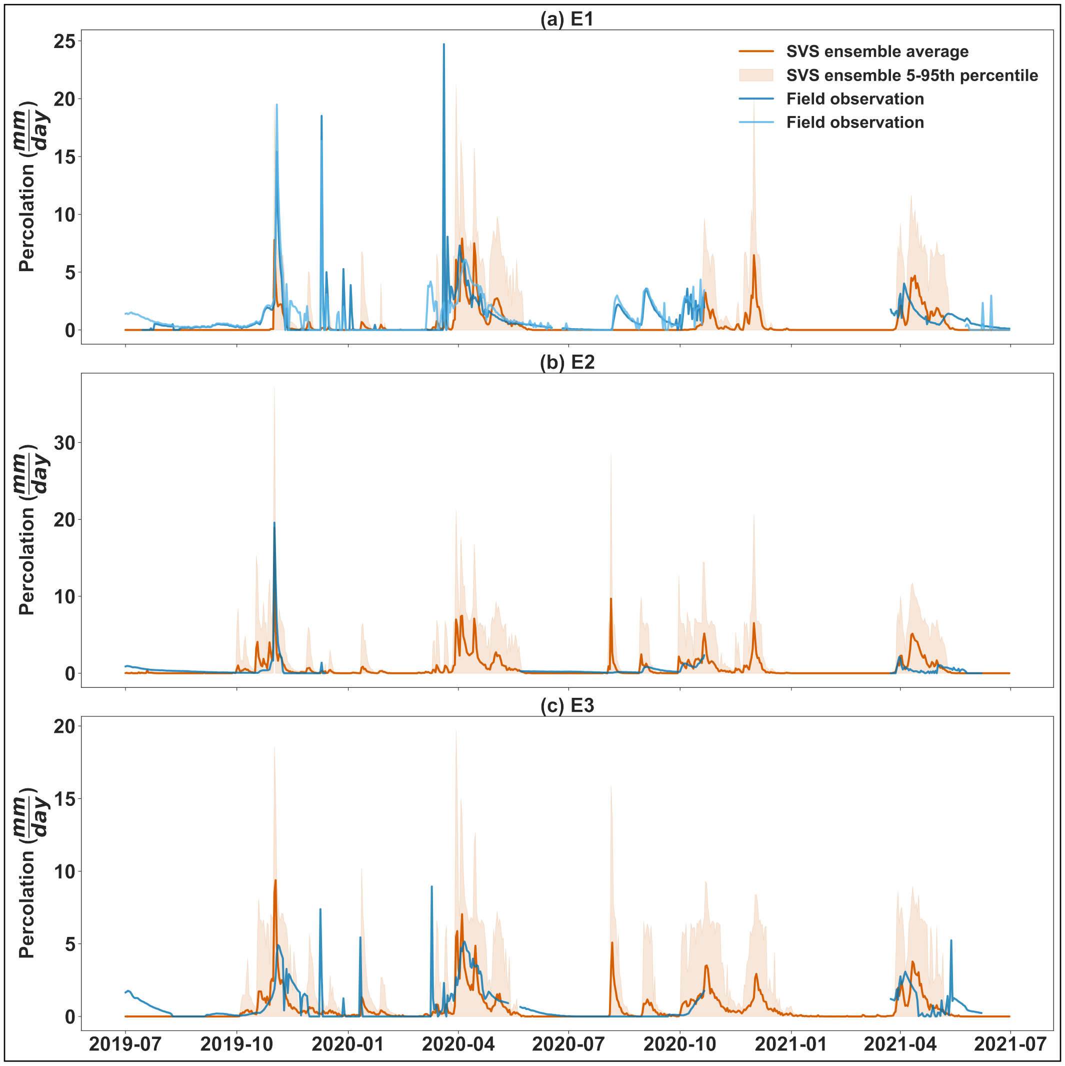

Figure 8: Total volume of daily percolation simulated by SVS (in orange, with the ensemble mean and the 5-95th percentile range) and the measured quantities from the lysimeters (light/dark blue) situated at the bottom of the (a) E1, (b) E2, and (c) E3 plots. Two lysimeters were placed inside the E1 plot.

There are periods when measurements are not available due to issues with data loggers and drainage pipes. However, it is still possible to compare the simulated percolation volumes from SVS with the measured values. Figure 8 shows that most percolation is collected in spring after the snow melts or in fall.

In winter, the surface soil freezes, as indicated by sensors placed at 7.5 cm recording subzero temperatures, thereby reducing the amount of percolation collected from the experimental plots due to limited water infiltration. Data on percolation and near-surface soil temperature for the experimental plots from 2019-07 to 2021-07 reveals that, on average, only 2 % of the total percolation volume was collected during frozen periods. This underlines the necessity for accurate simulation of soil freeze-thaw cycles. Factors such as the reduced infiltration capacity of frozen ground (Heinze, 2021), the contraction of pore space and decrease in unsaturated hydraulic conductivity due to frozen trapped pore water, and the inverse correlation between water temperature and its dynamic viscosity, can partially account for the observed effect.

As shown in Figure 8, the percolation during fall is significantly higher than in summer, despite the average monthly total rainfall being roughly the same throughout both seasons (Jun to Nov, with an average of 94 mm per month). This may be attributed to evapotranspiration loss in summer (June to August), which can account for 65% of the total annual evapotranspiration on average in Canada, while the loss in the colder months (including October and November) can be less than 10 mm per month Wang et al. (2013).

The seasonality of percolation at the study location suggests that missing data in the fall or spring likely include significant percolation. For instance, the first period of missing data in the E2 experimental plot (Figure 8-c) includes spring 2020, when large volumes of percolation occurred in the other experimental plots. It is reasonable to assume that similar percolation events also occurred in the E2 plot.

Figure 8 shows that SVS accurately matches the timing of major percolation events. In addition, the simulation accurately shows little or no percolation during winter and summer, consistent with observed patterns of percolation at the study location. However, Figure 8-a shows the model does not simulate percolation at all for two significant rainfall events in Aug 2020, which is collected by the lysimeter inside E1. While this highlights the need for further refinement of the SVS model, overall it demonstrates its ability to capture the seasonal and sub-seasonal patterns of percolation dynamics in the study area.

The CRPSS values for percolation from the plots, shown in Figure 4, are 0.13, -0.13, and 0.33. According to these values, SVS has acceptable performance for E1 and E3, while it performs worse than the benchmark for the E2 plot. However, this poor performance must be considered in light of the fact that major percolation volumes were not recorded in the spring of 2020 for the E2 plot, where SVS has simulated a significant amount of percolation.

The R^2 between the ensemble average and the daily percolation collected by the two lysimeters inside E1 is 0.15 and 0.24. Considering the fact that R^2 between the collected percolation by these two lysimeters is 0.56, it would not be unreasonable to consider the model's performance moderately successful. Concerning the E2 and E3 plots, the R^2 values are 0.46 and 0.28, which indicates the simulated percolation has a considerably higher correlation with observed values, compared to the case of E1. Assuming the same inherent variability for percolation from E2 and E3, as demonstrated by the fact that R^2 between two adjacent lysimeters can be as low as 0.56, we can argue that SVS has a good performance concerning E2 and E3, in terms of correlation.

Figure 8 shows that, for all plots, there is a large variability in the timing of the simulated percolation between the members of each ensemble. It is highly likely that the main source of variation in this regard is the wide sampling space for the ω_{trig} parameter, which is 50-99 % of ω_{sat} of cover material. This suggests that further refinement of the sampling space could potentially improve the performance of the ensemble simulations.

5. Conclusion

Reliable estimation of percolation is crucial for various applications, including landfill engineering, irrigation management, and groundwater management. Land-surface models offer a valuable tool for simulating percolation and enhancing our understanding of the complex interactions between soil properties, hydrological processes, and environmental factors.

We evaluate the ability of the SVS land-surface model to simulate percolation from the bottom of three experimental plots (soil covers) equipped with pan lysimeters, soil moisture, and temperature sensors. These plots are constructed at a landfill site in the vicinity of Drummondville, Quebec (Canada), with a warm-summer humid continental climate. The site receives a significant amount of snowfall during the cold months (Nov-Apr) and undergoes seasonal soil freeze-thaw cycles. This presents an opportunity to assess the performance of the newly developed soil-freezing module of SVS.

The main research question is the following: **are land-surface models (and in particular SVS) able to simulate percolation in a cold climate where the soil undergoes seasonal freeze-thaw cycles**? To address this, 200-member ensemble simulations are created for each plot, considering uncertainties in meteorological input data, soil hydraulic properties, and lower boundary condition associated with percolation simulations (i.e. trigger moisture). The simulation period spans from July 2018 to June 2021 (inclusively), with the first year used only for model warm-up.

To represent uncertainty in model input parameters, sampling intervals are created (by considering the ranges presented in Table 1) for each parameter with multiple laboratory-estimated values. For trigger moisture (ω_{trig}), an interval ranging from 0.5 to 0.99 of the corresponding soil layer's saturated water content (ω_{sat}) is defined. Meteorological data ensembles are constructed by applying a random perturbation to variables using a first-order autoregressive model (AR1) for physically consistent temporal variations.

The results demonstrate the ability of the SVS model to capture the seasonal and sub-seasonal patterns of percolation dynamics in the study area. The model accurately matches the timing of major percolation events due to snowmelt in spring and in fall and shows little or no percolation during winter and summer. The CRPSS values for the E1 and E3 plots indicate an acceptable model performance, while the performance for the E2 plot is worse than the benchmark. The R^2 values between the ensemble average and the daily percolation show a moderately successful to good model performance for the E1, E2, and E3 plots. It is worth noting that the correlation in percolation data between two closely located lysimeters is only around 0.56. This highlights the spatial variability and complexity of percolation processes in the field.

While SVS shows promise in its ability to simulate percolation dynamics, it also highlights certain shortcomings that need to be addressed. Specifically, inaccuracies in simulating soil freezing and soil moisture potentially contribute to percolation simulation errors. Overestimation of soil freezing duration by the model impacts the accurate simulation of water infiltration, thereby leading to an underestimation of soil moisture levels. An underestimation of soil moisture can translate into a reduced simulation of percolation. This is particularly consequential during critical periods of high infiltration such as snowmelt. Furthermore, discrepancies between the laboratory measurements of soil hydraulic parameters and their actual field values could also be contributing to the model's underestimation of soil moisture, thus affecting the prediction of percolation.

SVS simulates near-surface soil temperature dynamics reasonably well with CRPSS values of approximately 0.70 and R^2 values of approximately 0.98 for all three plots. However, the model may underestimate near-surface soil temperature and has limitations in simulating soil temperature for snow-free situations and air temperatures below the freezing point. There are large discrepancies between the onset, duration, and end of simulated and observed soil freezing periods, where SVS largely overestimates the duration of the freezing period. These dynamics are critical in simulating percolation and overland flow due to snowmelt events in spring. Therefore, further efforts are necessary to improve the model's accuracy in simulating soil freezing periods and their impacts on hydrological processes in snow-dominated regions.

Our findings underscore the SVS model's value and potential while emphasizing areas that require further improvement. Moving forward, future studies could consider using multiple models for soil water retention curves which may help account for uncertainty in the model's structure. Additionally, we can explore the applicability of the model to different geographical regions or climatic conditions.

Acknowledgements

This study was partly supported by the Natural Science and Engineering Research Council of Canada (NSERC) grants RGPIN-2019-06455 (2nd author). This work was supported by Natural Sciences and Engineering Research Council of Canada grant CRD # RDPJ_508222-16 and the Consortium de recherche et innovations en bioprocédés industriels du Québec - (CRIBIQ) grant CRIBIQ_2017-014-C27 (3rd author)

CONFLICT OF INTEREST STATEMENT

The authors declare no conflicts of interest.

DATA AVAILABILITY STATEMENT

All the codes required to reproduce the ensemble simulations, the evaluations, and figures, along with the SVS source code, are hosted at the following GitHub repository: `https://github.com/Alireza-Amani/SVS_percolation`. The datasets presented in this study are publicly available in the Zenodo repository and can be accessed at Cabral (2023). The repository contains daily percolation volumes and soil moisture and temperature measurements collected from experimental plots between July 1, 2018, and June 30, 2021. Readers are encouraged to utilize these data in their research with appropriate attribution.

References

Abdalla, M., Hastings, A., Cheng, K., Yue, Q., Chadwick, D., Espenberg, M., Truu, J., Rees, R. M., & Smith, P. (2019). A critical review of the impacts of cover crops on nitrogen leaching, net greenhouse gas balance and crop productivity. *Global change biology*, *25*, 2530–2543.

Alavi, N., Bélair, S., Fortin, V., Zhang, S., Husain, S. Z., Carrera, M. L., & Abrahamowicz, M. (2016). Warm season evaluation of soil moisture prediction in the soil, vegetation, and snow (svs) scheme. *Journal of hydrometeorology*, *17*, 2315–2332.

Ascott, M., Gooddy, D. C., Wang, L., Stuart, M. E., Lewis, M., Ward, R., & Binley, A. M. (2017). Global patterns of nitrate storage in the vadose zone. *Nature Communications*, *8*, 1–7.

Benson, C., Bohnhoff, G., Ogorzalek, A., Shackelford, C., Apiwantragoon, P., & Albright, W. (2005). Field data and model predictions for a monolithic alternative cover. In *Waste containment and remediation* (pp. 1–16).

Bethune, M., Selle, B., & Wang, Q. (2008). Understanding and predicting deep percolation under surface irrigation. *Water Resources Research*, *44*.

Bezerra-Coelho, C. R., Zhuang, L., Barbosa, M. C., Soto, M. A., Van Genuchten, M. T. et al. (2018). Further tests of the hyprop evaporation method for estimating the unsaturated soil hydraulic properties. *Journal of Hydrology and Hydromechanics*, *66*, 161–169.

Bhumralkar, C. M. (1975). Numerical experiments on the computation of ground surface temperature in an atmospheric general circulation model. *Journal of Applied Meteorology and Climatology*, *14*, 1246–1258.

Blackadar, A. K. (1976). Modelng the nocturnal boundary layer. In *Preprints, Third Symp. on Atmospheric Turbulence, Diffusion, and Air Quality, Raleigh*. Amer. Meteor. Soc.

Bohnhoff, G., Ogorzalek, A., Benson, C., Shackelford, C., & Apiwantragoon, P. (2009). Field data and water-balance predictions for a monolithic cover in a semiarid climate. *Journal of Geotechnical and Geoenvironmental Engineering*, *135*, 333–348.

Boone, A., Masson, V., Meyers, T., & Noilhan, J. (2000). The influence of the inclusion of soil freezing on simulations by a soil–vegetation–atmosphere transfer scheme. *Journal of Applied Meteorology and Climatology*, *39*, 1544–1569.

Bröcker, J., & Smith, L. A. (2007). Increasing the reliability of reliability diagrams. *Weather and forecasting*, *22*, 651–661.

Cabral, A. R. (2023). Daily Averaged Soil State Variables and Daily Percolation Volumes from Three Experimental Plots (Soil Covers): 2018-2021. Zenodo. URL: `https://doi.org/10.5281/zenodo.7948797`. doi:`10.5281/zenodo.7948797`.

Carpenter, S. R., Caraco, N. F., Correll, D. L., Howarth, R. W., Sharpley, A. N., & Smith, V. H. (1998). Nonpoint pollution of surface waters with phosphorus and nitrogen. *Ecological applications*, *8*, 559–568.

Charrois, L., Cosme, E., Dumont, M., Lafaysse, M., Morin, S., Libois, Q., & Picard, G. (2016). On the assimilation of optical reflectances and snow depth observations into a detailed snowpack model. *The Cryosphere*, *10*, 1021–1038.

Clapp, R. B., & Hornberger, G. M. (1978). Empirical equations for some soil hydraulic properties. *Water resources research*, *14*, 601–604.

Clark, E. A. (2017). Particle Filter data assimilation of streamflow in basins with seasonal snow for initializing short-to medium-range streamflow forecasts.

Colli, M., Lanza, L., & Chan, P. (2013). Co-located tipping-bucket and optical drop counter ri measurements and a simulated correction algorithm. *Atmospheric Research*, *119*, 3–12.

Deodatis, G., & Shinozuka, M. (1988). Auto-regressive model for nonstationary stochastic processes. *Journal of engineering mechanics*, *114*, 1995–2012.

Fayer, M. J. (2000). *UNSAT-H version 3.0: Unsaturated soil water and heat flow model theory, user manual, and examples*. Technical Report Pacific Northwest National Lab.(PNNL), Richland, WA (United States).

Finch, J. (1998a). Estimating direct groundwater recharge using a simple water balance model–sensitivity to land surface parameters. *Journal of Hydrology*, *211*, 112–125.

Finch, J. (1998b). Estimating direct groundwater recharge using a simple water balance model–sensitivity to land surface parameters. *Journal of Hydrology*, *211*, 112–125.

Fu, Q., Hou, R., Li, T., Jiang, R., Yan, P., Ma, Z., & Zhou, Z. (2018). Effects of soil water and heat relationship under various snow cover during freezing-thawing periods in songnen plain, china. *Scientific Reports*, *8*, 1–12.

Ganji, A., Sushama, L., Verseghy, D., & Harvey, R. (2017). On improving cold region hydrological processes in the canadian land surface scheme. *Theoretical and Applied Climatology*, *127*, 45–59.

Hayashi, M., Goeller, N., Quinton, W. L., & Wright, N. (2007). A simple heat-conduction method for simulating the frost-table depth in hydrological models. *Hydrological Processes: An International Journal*, *21*, 2610–2622.

He, H., Liu, L., Dyck, M., Si, B., & Lv, J. (2021). Modelling dry soil thermal conductivity. *Soil and Tillage Research*, *213*, 105093.

Heinze, T. (2021). A multi-phase heat transfer model for water infiltration into frozen soil. *Water Resources Research*, *57*, e2021WR030067.

Hersbach, H. (2000). Decomposition of the continuous ranked probability score for ensemble prediction systems. *Weather and Forecasting*, *15*, 559–570.

Hersbach, H., Bell, B., Berrisford, P., Hirahara, S., Horányi, A., Muñoz-Sabater, J., Nicolas, J., Peubey, C., Radu, R., Schepers, D. et al. (2020). The era5 global reanalysis. *Quarterly Journal of the Royal Meteorological Society*, *146*, 1999–2049.

Husain, S. Z., Alavi, N., Bélair, S., Carrera, M., Zhang, S., Fortin, V., Abrahamowicz, M., & Gauthier, N. (2016). The multibudget soil, vegetation, and snow (svs) scheme for land surface parameterization: Offline warm season evaluation. *Journal of Hydrometeorology*, *17*, 2293–2313.

Hutson, J., & Wagenet, R. (1995). An overview of leachm: a process based model of water and solute movement, transformations, plant uptake and chemical reactions in the unsaturated zone. *Chemical equilibrium and reaction models*, *42*, 409–422.

Iwata, Y., Hayashi, M., Suzuki, S., Hirota, T., & Hasegawa, S. (2010). Effects of snow cover on soil freezing, water movement, and snowmelt infiltration: A paired plot experiment. *Water resources research*, *46*.

Jennings, K. S., Winchell, T. S., Livneh, B., & Molotch, N. P. (2018). Spatial variation of the rain–snow temperature threshold across the northern hemisphere. *Nature communications*, *9*, 1–9.

Johansen, O. (1975). Varmeledningsevne av jordarter (thermal conductivity of soils). *CRREL Draft English Translation*, *637*.

Kahale, T., & Cabral, A. R. (2022). Field and numerical evaluation of breakthrough suction effects in lysimeter design. *Environmental Technology*, *0*, 1–14. URL: `https://doi.org/10.1080/09593330.2022.2139635`. doi:`10.1080/09593330.2022.2139635`. `arXiv:https://doi.org/10.1080/09593330.2022.2139635`. PMID: 36274583.

Kjeldsen, P., Barlaz, M. A., Rooker, A. P., Baun, A., Ledin, A., & Christensen, T. H. (2002). Present and long-term composition of msw landfill leachate: a review. *Critical reviews in environmental science and technology*, *32*, 297–336.

Krahn, J. (2004). Vadose zone modeling with vadose/w: An engineering methodology. *GEO-SLOPE International Ltd, Calgary, Alberta, Canada*, .

Kurylyk, B. L., & Watanabe, K. (2013). The mathematical representation of freezing and thawing processes in variably-saturated, non-deformable soils. *Advances in Water Resources*, *60*, 160–177.

Lanza, L., Leroy, M., Alexandropoulos, C., Stagi, L., & Wauben, W. (2005). Laboratory intercomparison of rainfall intensity gauges. *World Meteorological Organisation–Instruments and Observing Methods Rep*, *84*.

Leonardini, G., Anctil, F., Abrahamowicz, M., Gaborit, É., Vionnet, V., Nadeau, D. F., & Fortin, V. (2020). Evaluation of the soil, vegetation, and snow (svs) land surface model for the simulation of surface energy fluxes and soil moisture under snow-free conditions. *Atmosphere*, *11*, 278.

Leonardini, G., Anctil, F., Vionnet, V., Abrahamowicz, M., Nadeau, D. F., & Fortin, V. (2021). Evaluation of the snow cover in the soil, vegetation, and snow (svs) land surface model. *Journal of Hydrometeorology*, . doi:10.1175/jhm-d-20-0249.1.

Loh, W.-L. (1996). On latin hypercube sampling. *The annals of statistics*, *24*, 2058–2080.

Maheu, A., Anctil, F., Gaborit, É., Fortin, V., Nadeau, D. F., & Therrien, R. (2018). A field evaluation of soil moisture modelling with the soil, vegetation, and snow (svs) land surface model using evapotranspiration observations as forcing data. *Journal of Hydrology*, *558*, 532–545.

Mijares, R. G., & Khire, M. V. (2012). Field data and numerical modeling of water balance of lysimeter versus actual earthen cap. *Journal of geotechnical and geoenvironmental engineering*, *138*, 889–897.

Mohammed, G. A., Hayashi, M., Farrow, C. R., & Takano, Y. (2013). Improved characterization of frozen soil processes in the versatile soil moisture budget model. *Canadian Journal of Soil Science*, *93*, 511–531.

Niu, G.-Y., & Yang, Z.-L. (2006). Effects of frozen soil on snowmelt runoff and soil water storage at a continental scale. *Journal of Hydrometeorology*, *7*, 937–952.

Niu, G.-Y., & Yang, Z.-L. (2007). An observation-based formulation of snow cover fraction and its evaluation over large north american river basins. *Journal of geophysical research: Atmospheres*, *112*.

Peel, M. C., Finlayson, B. L., & McMahon, T. A. (2007). Updated world map of the köppen-geiger climate classification. *Hydrology and earth system sciences*, *11*, 1633–1644.

Peters-Lidard, C., Blackburn, E., Liang, X., & Wood, E. F. (1998). The effect of soil thermal conductivity parameterization on surface energy fluxes and temperatures. *Journal of the Atmospheric Sciences*, *55*, 1209–1224.

Rooney, E. C., Bailey, V. L., Patel, K. F., Dragila, M., Battu, A. K., Buchko, A. C., Gallo, A. C., Hatten, J., Possinger, A. R., Qafoku, O. et al. (2022). Soil pore network response to freeze-thaw cycles in permafrost aggregates. *Geoderma*, *411*, 115674.

Schindler, U., von Unold, G., Durner, W., & Mueller, L. (2015). Recent progress in measuring soil hydraulic properties. In *Proceedings of the International Conference on Environment and Civil Engineering* (pp. 24–25).

Schindler, U. G., & Müller, L. (2017). Soil hydraulic functions of international soils measured with the extended evaporation method (eem) and the hyprop device. *Open Data Journal for Agricultural Research*, *3*.

Simunek, J., Van Genuchten, M. T., & Sejna, M. (2005). The hydrus-1d software package for simulating the one-dimensional movement of water, heat, and multiple solutes in variably-saturated media. *University of California-Riverside Research Reports*, *3*, 1–240.

Smith, C. D., Mekis, E., Hartwell, M., & Ross, A. (2022). The hourly wind-bias-adjusted precipitation data set from the environment and climate change canada automated surface observation network (2001–2019). *Earth System Science Data*, *14*, 5253–5265.

Smith, V. H., Joye, S. B., & Howarth, R. W. (2006). Eutrophication of freshwater and marine ecosystems. *Limnology and oceanography*, *51*, 351–355.

Verseghy, D. L. (1991). Class—a canadian land surface scheme for gcms. i. soil model. *International Journal of Climatology*, *11*, 111–133.

Wang, H., Tetzlaff, D., & Soulsby, C. (2018). Modelling the effects of land cover and climate change on soil water partitioning in a boreal headwater catchment. *Journal of Hydrology*, *558*, 520–531.

Wang, P., Song, X., Han, D., Zhang, Y., & Zhang, B. (2012). Determination of evaporation, transpiration and deep percolation of summer corn and winter wheat after irrigation. *Agricultural Water Management*, *105*, 32–37.

Wang, S., Yang, Y., Luo, Y., & Rivera, A. (2013). Spatial and seasonal variations in evapotranspiration over canada's landmass. *Hydrology and Earth System Sciences*, *17*, 3561–3575.

Xu, B., Shao, D., Tan, X., Yang, X., Gu, W., & Li, H. (2017). Evaluation of soil water percolation under different irrigation practices, antecedent moisture and groundwater depths in paddy fields. *Agricultural Water Management*, *192*, 149–158.

Xu, W., Li, K., Chen, L., Kong, W., & Liu, C. (2021). The impacts of freeze–thaw cycles on saturated hydraulic conductivity and microstructure of saline–alkali soils. *Scientific Reports*, *11*, 1–15.

Zhao, L., Gray, D. M., & Male, D. H. (1997). Numerical analysis of simultaneous heat and mass transfer during infiltration into frozen ground. *Journal of Hydrology*, *200*, 345–363.

Appendix A. Soil freezing module in SVS

SVS uses a hybrid approach that combines Force Restore schemes to compute the surface energy budget of bare ground, vegetation, and snow (Husain et al., 2016) with a multi-layer hydrological module solving the Richards equations for unsaturated flow in a porous media Alavi et al. (2016). This hybrid approach initially prevented the simulation of soil freezing and thawing by the model. To overcome this limitation a new module has been developed.

The representation of soil freezing in SVS relies on the soil freezing/thawing module available in the Versatile Soil Budget Model (VSMB Mohammed et al., 2013). This module is based on the simple heat-conduction algorithm of Hayashi et al. (2007) and simulates the evolution of soil temperature and associated phase changes without the computationally expensive iterative solution of coupled non-linear equations. In SVS, soil temperature, and phase changes are solved on the same vertical grid as the hydrological processes using upper boundary conditions provided by the force restore schemes solving the multiple energy budgets at the surface (Husain et al., 2016).

Appendix A.1. Heat conduction algorithm

In the soil temperature algorithm, the heat conduction between two adjacent soil layers (upper to lower) is given by:

$$q_h = -\lambda_s \frac{\Delta_z T}{\Delta z} \tag{A.1}$$

where q_h is the soil heat flux (W m^{-2}), $\Delta_z T$ is the difference in soil temperature between adjacent layers (lower minus upper) (K), Δz is the distance between the centers of the (m) and λ_s is the bulk thermal conductivity given by the thickness-weighted harmonic mean conductivity of the two layers (W K^{-1} m^{-1}).

For a given soil layer j, the net heat flux ($\Delta_z q_{h,j}$) is then computed as:

$$\Delta_z q_{h,j} = q_{h,j-1} - q_{h,j} \tag{A.2}$$

The soil temperature algorithm assumes then that the change in net heat flux corresponds to a change in heat stored as sensible and latent heat in layer j:

$$\Delta_z q_{h,j} = (\Delta_t T_j c_{s,j} + \Delta_t w_{i,j} \rho_w L_f) d_j \tag{A.3}$$

where $\Delta_t T_j$ (K) and $\Delta_t w_{i,j}$ (kg kg^{-1}) are the changes in soil temperature and liquid equivalent ice content of layer j, respectively, with time, ρ_w is the density of water (kg m^{-3}), L_f is the latent heat of fusion (J kg^{-1}), d_j is the layer thickness (m), and $c_{s,j}$ is the volumetric heat capacity of the soil layer (J m^{-3} K^{-1}).

The VSMB soil freezing scheme assumes that water in soil pores freezes at T_{ref} = 273.15 K and ignores the freezing-point depression (Kurylyk & Watanabe, 2013). It accounts for the presence of unfrozen water that remains in the soil at sub-zero temperatures and co-exists with ice. The default VSMB algorithm assumes that the residual unfrozen water content, $w_{l,r}$, is constant and equals 0.06. This option has been used in the work since it corresponds well to local observations of residual liquid water content in frozen conditions. Another option in SVS allows the unfrozen residual water content to depend on the soil texture based on Niu & Yang (2006). If a soil layer j is completely thawed or frozen with no liquid water above the residual frozen water content (i.e., $T_j \neq T_{ref}$), $\Delta_z q_{h,j}$ is converted to sensible heat until T_j reaches T_{ref} and any residual is converted to latent heat (melting of freezing). If the soil is already frozen (T_j=T_{ref}), $\Delta_z q_{h,j}$ is first used for phase change of all available liquid water above $w_{l,r}$ and any residual is converted to sensible heat. Calculations are performed sequentially from the top to the lowest soil layer.

The thermal heat capacity, c_s, and thermal conductivity, λ_s, of the soil layers are parameterized following Peters-Lidard et al. (1998) as functions of soil moisture and texture (percentage of sand and clay) and account for the effect frozen soils as described in Boone et al. (2000). The dry soil thermal conductivity and soil thermal conductivity are taken from He et al. (2021) and Johansen (1975), respectively.

Appendix A.2. Lower boundary condition

The heat flux at the bottom of the lowest soil layer is specified using an annual mean deep soil temperature, T_{btm}, and an appropriate scaling depth, z_{btm}. It is written as:

$$q_{h,N} = \lambda_{s,N} \frac{T_N - T_{btm}}{(z_{btm} - z_N)} \tag{A.4}$$

where N corresponds to the deepest soil layer. In this study, T_{btm} was set to 7.5 (°C) and z_{btm} set to 5 m.

Appendix A.3. Upper boundary condition

The upper boundary condition accounts for the surface tiling use in SVS and includes the contribution from: (i) snow-free bare ground, (ii) snow-free low and high vegetation, (iii) snow over bare ground and low vegetation, and (iv) snow below high vegetation. The heat flux at the top of the superficial soil layer is written as:

$$q_{h,0} = (1-f_{veg}) \left[(1 - f_{snw})H_{grnd} + f_{snw}H_{snw}\right] + f_{veg} \left[(1 - f_{snwv})H_{veg} + f_{snwv}H_{snwv}\right] \tag{A.5}$$

Where f_{veg}, f_{snw} and f_{snwv} are the fractions of the grid cell covered by high vegetation, the fraction of low vegetation and the bare ground covered by snow, and the fraction of soil under high-vegetation covered by snow, respectively. H_{grnd}, H_{veg}, H_{snw} and H_{snwv} are the heat flux (W m^{-2}) from snow-free bare ground, snow-free vegetation, snow over bare ground and low vegetation and snow below high vegetation.

For bare ground, the heat flux depends on the difference between the skin-temperature T_{gs} simulated by the force-restore approach for bare ground and the temperature of the upper soil layer (j=1). It is written as:

$$H_{grnd} = \frac{T_{gs} - T_1}{R_g} \text{ with } R_g = \frac{d_1}{2\lambda_{s,1}} \tag{A.6}$$

In its current version, the soil freezing scheme has no feedback on the force restore scheme used for bare ground. Therefore, the prognostic temperature variables of the force restore scheme used for bare ground lack the effect of latent heat release due to soil freezing and thawing. This can lead to an underestimation of soil temperature during soil freezing and an overestimation of soil temperature during soil thawing.

SVS does not simulate the evolution of the surface soil temperature below the low and high vegetation. This limits the ability to compute accurately the heat flux below the vegetation tile. For this reason, without more information available, the heat flux from the vegetation tile is assumed to be the same as the heat flux from the bare ground tile: $H_{veg} = H_{grnd}$.

The force restore schemes used for the snowpack over bare ground and low vegetation and the snowpack below high vegetation do not provide information on the temperature at the interface between the ground and the snow. Therefore, the deep snow temperature, $T_{snw,d}$, from the force restore scheme is used to estimate the heat flux between the superficial soil layer and the snow. It is written as:

$$H_{snw} = \frac{T_{snw,d} - T_1}{R_{snw}} \text{ with } R_{snw} = \frac{h_{therm}}{\lambda_{snw}} + \frac{d_1}{2\lambda_{s,1}} \tag{A.7}$$

where λ_{snw} is the snow thermal conductivity (W m^{-1} K-$^{-1}$) and h_{therm} the thickness used to compute the thermal exchanges between the snowpack and the ground (m). h_{therm} depends on the snow damping depth, d_{snw}, used to characterize the diurnal variation of temperature close to the snow surface in the Force Restore scheme (Leonardini et al., 2021). h_{therm} is computed as $h_{therm} = \max/(h_{snw}/2, h_{snw} - d_{snw})$ where h_{snw} is the total snow depth. The heat flux between the superficial soil layer and the snowpack below high vegetation,

H_{snwv}, is derived in the same way as H_{snw} using the simulated information for the snowpack below high vegetation.

An accurate estimation of the fraction of the soil covered by snow is an important component of the soil freezing scheme. Indeed, it affects the estimation of the surface heat flux and strongly controls soil freezing in the fall and soil thawing in springtime. Two approaches can be used for snow cover fraction in the soil freezing scheme. For the first option, the fraction is computed as f_{snw}= max/(1., $\frac{\rho_{snw} h_{snw}}{W_{cr}}$) with $W_{cr} = 1$ kg m^{-2}. The same formulation is used for f_{snwv}. With this formulation, the snow cover fraction reaches the value of 1 as soon as the snow is present on the ground. Such formulation is mainly suitable for point-scale applications of the soil freezing scheme and was used in the study. A second option, recommended for gridded simulations, relies on the formulation of Niu & Yang (2007):

$$f_{snw} = f_{snwv} = \tanh/\left(\frac{h_{snw}}{2.5 z_0 \left(\frac{\rho_{snw}}{\rho_{ref}}\right)^m}\right) \tag{A.8}$$

where $\rho_{ref} = 100$ kg m^{-3} and m = 1.6 are the default values from Niu & Yang (2007). In the soil freezing scheme, z_0 is set to 0.01 m to preserve a rapid increase of the snow cover fraction with snow depth. The term $\left(\frac{\rho_{snw}}{\rho_{ref}}\right)^m$ in the denominator aims at roughly representing the hysteresis associated with the snow cover fraction (Niu & Yang, 2007).

Appendix A.4. Hydrological impact

The presence of frozen soil ($w_i > 0$) modifies the hydraulic conductivity at saturation and the soil porosity in the SVS soil hydrology scheme. The saturated hydraulic conductivity in the presence of frozen soil is written as $k_{satc} = f_{ice} k_{sat}$ where k_{sat} is the hydraulic conductivity at saturation that depends on soil texture. f_{ice} is a parameter that aims are reducing k_{sat} in presence of frozen water in the soil (e.g., Kurylyk & Watanabe, 2013). It is computed as in the CLASS land surface scheme (Ganji et al., 2017):

$$f_{ice} = \left[1 - \max/\left(0, \min/\left(\frac{w_{sat} - 0.001}{w_{sat}}, \frac{w_i}{w_{sat}}\right)\right)\right]^2 \tag{A.9}$$

where w_{sat} is the saturated volumetric water content.

The volumetric liquid water content at saturation is also reduced assuming that frozen water becomes part of the soil matrix (Zhao et al., 1997):

$$w_{satc} = \max/(0.001, w_{sat} - w_i) \tag{A.10}$$

Evapotranspiration is also indirectly impacted due to the change in the liquid water content when freezing and thawing occur.